ISSN 1063-7761, Journal of Experimental and Theoretical Physics, 2019, Vol. 129, No. 1, pp. 86–96. © Pleiades Publishing, Inc., 2019.
Russian Text © The Author(s), 2019, published in Zhurnal Eksperimental'noi i Teoreticheskoi Fiziki, 2019, Vol. 156, No. 1, pp. 105–117.

ORDER, DISORDER, AND PHASE TRANSITION IN CONDENSED SYSTEM

The Effect of Nonisothermality on the Early Stages of Spinodal Decomposition

V. G. Lebedev[a,b,*] and P. K. Galenko[c,d,]**

[a] *Institute of Mathematics, Information Technologies and Physics, Udmurt State University, Izhevsk, 426034 Russia*
[b] *Udmurt Federal Research Center, Ural Branch, Russian Academy of Sciences, Izhevsk, 426067 Russia*
[c] *Friedrich-Schiller-Universität Jena, Physikalisch–Astronomische Fakultät, D-07743 Jena, Germany*
[d] *Laboratory of Multi-Scale Mathematical Modeling, Ural Federal University, Yekaterinburg, 620002 Russia*
**e-mail: lvg@udsu.ru*
***e-mail: Peter.Galenko@uni-jena.de*

Received September 27, 2018; revised January 7, 2019; accepted January 10, 2019

Abstract—A nonisothertmal model of spinodal decomposition is proposed for a binary system described by the Ginzburg–Landau energy. The initial stages of spinodal decomposition are investigated for a system of simultaneous equations describing the impurity and temperature redistribution. The dispersion equation and the instability growth rate of spinodal structures are obtained. The temperature dependence of the growth rate and the wave number corresponding to the maximum instability is found. The observed difference in the dispersion relations of isothermal and nonisothermal models shows that a criterion for the effect of temperature fluctuations on the spinodal decomposition is given by a dimensionless parameter Γ; for large values of Γ ($\Gamma \geq 1000$), temperature fluctuations in the form of noise are certainly insufficient for spinodal decomposition due to a change in the dispersion structure of the equations, which suggests the need to take into account the nonisothermal behavior of the system.

DOI: 10.1134/S1063776119050030

1. INTRODUCTION

The processes of spontaneous separation of condensed media into regions with different impurity compositions, called spinodal decomposition, have been widely known since the 1950s. Spinodal decomposition has been observed in many experiments on polymer blends [1], liquid solutions [2, 3], and metal systems [4]. A phenomenological description of the phenomenon under isothermal conditions was proposed by Cahn and Hilliard [5, 6] and was theoretically developed and experimentally tested in [7–10]. It turned out [11, 12] that the experimental data do not always agree with the linear behavior of the dispersion relation in the Cahn–Hilliard model [5, 6]. It was noted [10] that the linear behavior of the dispersion relation at early stages of spinodal decomposition is characteristic of systems with long-range interaction, whereas, for systems with short-range interaction, nonlinear effects are essential [13, 14]. Today, the understanding of the physical nature of the early stages of spinodal decomposition is the main problem in the theory of this phenomenon. As regards the late stages of spinodal decomposition, when the separation of solutions into regions with different concentrations has already occurred, starting from [15], the authors were mainly focused on the description of the scenarios of coalescence and possible crossover between these regions. Since the natures of the phenomena at the initial and final stages of spinodal decomposition are significantly different, below we restrict the analysis to the initial stages of the process.

The nonlinearity at early stages can be attributed to the local nonequilibrium of the spinodal decomposition process [16–21], to the Brownian motion [22], as well as to the nonisothermality of the process in solutions. Most of the theoretical work on spinodal decomposition uses the so-called isothermal approximation. This approximation within a continuum model usually implies that the temperature of the system may vary with time, but at any moment it remains homogeneous in space. Within this work, speaking of non-isothermal spinodal decomposition, we will further assume that the temperature distribution is nonuniform and varies both in space and in time.

Earlier, temperature fluctuations were introduced into the spinodal decomposition process in [7, 8]. In [23], nonisothermality during the phase separation was taken into account in connection with the thermal expansion and the effect of elastic stresses on the spinodal decomposition in solid solutions. More modern approaches to the construction of a nonisothermal model of spinodal decomposition were pro-

posed in [24, 25]. However, these works contain no qualitative analysis of the dynamics of the proposed models. Therefore, at the moment, it is important to understand the nature and degree of influence of nonisothermality on spinodal decomposition. A numerical study of spinodal decomposition on the basis of the Cahn–Hilliard model in the presence of both the temperature dependence of the thermodynamic potential and random thermal noise was carried out in [26], where the authors demonstrated the effect of nonisothermality on the position of the extrema of the correlation function. In the present study, we propose a self-consistent thermodynamic description of nonisothermal spinodal decomposition on the basis of the approach of [27] and carry out a semianalytical analysis of the initial stages of decomposition for a temperature-dependent model binary system (solution) with the Ginzburg–Landau energy.

2. THE LANGER–BARON–MILLER (LBM) MODEL

The Langer–Baron–Miller (LBM) model describes spinodal decomposition at the initial instant of time and begins with the Cahn–Hilliard–Cook (CHC) equation [5–7]

$$\frac{\partial x}{\partial t} = M_D \nabla^2 \left(\frac{\delta \mathcal{F}}{\delta x} \right) + \xi(\mathbf{r}, t), \tag{1}$$

where ∇ is the gradient operator, $x(\mathbf{r}, t)$ is a local deviation from the mean value of the concentration of the impurity component in a binary solution, M_D is a positive transport coefficient (mobility) related to the diffusion coefficient of the impurity component, $\xi(\mathbf{r}, t)$ is thermal noise, and $\mathcal{F}$ is the total free energy of the system,

$$\mathcal{F} = \int \left(f(x) + \frac{1}{2}\varepsilon^2 (\nabla x)^2 \right) dV_0, \tag{2}$$

where dV_0 is a spatial volume element occupied by the solution. The coefficient ε^2 proportional to the squared correlation length for concentration fluctuations in the solution [5] and the free energy density $f(x)$ are determined by the equilibrium properties of the binary system. The expression $\varepsilon^2(\nabla x)^2$ in the Cahn–Hilliard theory describes the contribution of the interface energy between regions with different concentrations. If $f(x)$ has a single minimum, then Eq. (1) reduces to a diffusion equation with the characteristic dispersion relation [9]

$$\omega = -k^2 (D_0 + M_D \varepsilon^2 k^2)$$

between frequency ω and wave number k, where the contribution of the gradient term is assumed to be small compared with the diffusion coefficient $D_0 \equiv M_D(\partial^2 f(x)/\partial x^2)$:

$$M_D \varepsilon^2 k^2 \ll D_0.$$

The division into regions with different concentrations according to the spinodal decomposition mechanism occurs if $f(x)$ has two minima. Then, in the domain between the minima, the diffusion coefficient is negative ($D_0 < 0$), and the term with k^4 in the dispersion relation $\omega = k^2(|D_0| - M_D\varepsilon^2 k^2)$ limits the growth of short-wave perturbations, which points to the stabilizing role of the contribution $\varepsilon^2(\nabla x)^2$ in expression (2).

The CHC equation (1) in the LBM approach [8] is considered as a set of Langevin equations with an independent random source $\xi(\mathbf{r}, t)$ at every point of the space. Since the set of Langevin equations is equivalent to the Fokker–Planck equation for probability distribution [28], in [8], the authors made certain assumptions concerning the structure of this probability distribution, which made it possible to obtain the equation of motion for the structure factor $S(k, t)$, which is the Fourier transform of the simultaneous pair correlation function $\langle x(\mathbf{r}_1, t)x(\mathbf{r}_2, t)\rangle$ with respect to the difference $\mathbf{r}_1 - \mathbf{r}_2$. The evolution of the structure factor was compared with light scattering experiments in binary liquids [29]. Since the system was transferred to an unstable state through the removal of pressure, the LBM model well describes the resulting structure factors if we take into account that the process is adiabatic [30]. An exception is made by the initial moments of time when the theoretical curve lags behind the experimental curve. Somewhat later, the LBM theory was quantitatively confirmed by X-ray scattering at early stages of spinodal decomposition in $Al_{0.62}Zn_{0.38}$ solid solution in [31]. However, there is still no definite answer to the question of what is responsible for the discrepancy, found in [30], between theoretical and experimental data on the structure factor at the initial instants of time.

As the factors responsible for the discrepancy between theoretical and experimental data on the structure factor, one considered the local nonequilibrium of the spinodal decomposition process [16–21] at the initial instants of time, due to the flux relaxation. Phenomenologically, the dynamics of fluxes depends on their relaxation time, whose variation leads to a characteristic behavior of the growth rate of unstable modes [19, 20]. A complete quantitative description of the experimental data of [10–12] can be obtained only as a result of the comparative analysis of the effects of local nonequilibrium, nonisothermality, and Brownian motion. In this paper, we discuss the effect of nonisothermality of a process on the spinodal decomposition by an example of a simple thermodynamic model. The effect of Brownian motion requires separate consideration.

3. COMPUTER SIMULATION

After the formulation of the LBM model [8], its analysis, and the comparison of its solutions with experimental data [29, 30], the process of spinodal

decomposition has been intensively studied by methods of mathematical modeling [21] with regard to the extension of the thermodynamic description [18, 32] and with the application of the results in materials science [33, 34]. In this regard, note that the LBM model formally ignores the dynamics of the order parameter and directly describes the dynamics of the structure factor; this facilitates the analysis of the latter dynamics when processing the experimental data and offers two options for direct modeling:

(1) modeling the CHC equation (1) with noise and averaging the result for specific implementations;

(2) modeling the Fokker–Plank equation and finding the correlation functions (including the structure factor) by the distribution function obtained.

In practice, both approaches (1) and (2) are not usually used because the CHC equation is modeled either without any thermal noise [35–38] or with thermal noise [39–41] but without averaging over possible implementations.

There are many reasons for this difference between the approaches; on the whole, we can state that the paradigms of computer simulation and theoretical description of spinodal decomposition differ significantly from each other. Naturally, the question arises of how to bring them together as closely as possible. In this sense, the study of the effect of nonisothermality on spinodal decomposition is very important: the interaction between temperature and concentration should change the dispersion structure of the equations, thus leading to a single model instead of a two-faced Janus. Therefore, we briefly consider the derivation of a nonisothermal model of spinodal decomposition and analyze the dispersion relation of the model in comparison with the Cahn–Hilliard equation.

4. MODIFICATION OF THE CAHN–HILLIARD MODEL

For a simplified derivation of the Cahn–Hilliard model under nonisothermality conditions, we neglect locally nonequilibrium effects that take into account the flux relaxation [16–21]. This means that nonuniform temperature variations are considered at time intervals greater than the characteristic relaxation times of diffusion fluxes.

Consider the simplest system that describes spinodal decomposition and, at the same time, allows one to take into account the nonisothermality of the process. Due to additivity, the Gibbs potential of the total system should consist of the bulk potential and the energy of the interface between regions with different concentrations $x(\mathbf{r}, t)$. Denote the temperature field by $T(\mathbf{r}, t)$. Assume that the problem is isobaric, with pressure equal to zero. As the control functional of a nonisothermal, isobaric system, we take the entropy of the system,

$$S = -\int\left(\frac{\partial G}{\partial T} + \frac{\varepsilon^2}{2T_0}(\nabla x)^2\right)dV_0, \tag{3}$$

where $G = G(T, x)$ is the Gibbs potential density and T_0 is the temperature of the initial state of the solution.

Neglecting the variation of the volume and internal stresses during spinodal decomposition and expressing the enthalpy density $H(x, T)$ in terms of the Gibbs potential density $G(x, T)$,

$$H = G - T\frac{\partial G}{\partial T}, \tag{4}$$

we write the enthalpy conservation law

$$\frac{\partial H}{\partial t} = -\nabla\cdot\mathbf{J}_T, \tag{5}$$

where $\mathbf{J}_T$ is the heat flux. Using expression (4) and calculating the partial derivatives of a composite function, we rewrite Eq. (5) as

$$\frac{\partial T}{\partial t}\frac{\partial^2 G}{\partial T^2} + \frac{\partial x}{\partial t}\frac{\partial^2 G}{\partial T\partial x} = \frac{1}{T}\left(\nabla\cdot\mathbf{J}_T + \frac{\partial x}{\partial t}\frac{\partial G}{\partial x}\right). \tag{6}$$

Since the specific heat at constant pressure is $C_p = -T(\partial^2 G/\partial T^2)$, we define the chemical potential as $\mu = (\partial G/\partial x)$ and pass from relation (6) to the heat equation

$$C_p\frac{\partial T}{\partial t} = -\nabla\cdot\mathbf{J}_T + T^2\frac{\partial x}{\partial t}\frac{\partial}{\partial T}\left(\frac{\mu}{T}\right). \tag{7}$$

On the other hand, the differentiation of entropy (3) with respect to time can be reduced, with the use of relation (6), to the expression

$$\frac{dS}{dt} = -\int\left[\frac{1}{T}\nabla\cdot\mathbf{J}_T + \left(-\frac{\mu}{T} + \frac{\varepsilon^2}{T_0}\nabla^2 x\right)\frac{\partial x}{\partial t}\right]dV_0. \tag{8}$$

Using the impurity conservation law

$$\frac{\partial x}{\partial t} = -\nabla\cdot\mathbf{J}_D, \tag{9}$$

where $\mathbf{J}_D$ is the diffusion flux, we can rewrite (8) as

$$\frac{dS}{dt} = \int\left[\mathbf{J}_T\cdot\nabla\left(\frac{1}{T}\right) - \mathbf{J}_D\cdot\nabla\left(\frac{\mu}{T} - \frac{\varepsilon^2}{T_0}\nabla^2 x\right)\right]dV_0. \tag{10}$$

Using the available freedom in the definition of fluxes [42] and separating total squares in (10), we obtain the following expression for fluxes from the condition of nonnegativity of entropy variation in relaxation processes ($dS/dT \geq 0$):

$$\mathbf{J}_T = -\frac{M_T}{T^2}\nabla T = -\lambda\nabla T, \tag{11}$$

where λ is the thermal diffusivity of the solution and

$$\mathbf{J}_D = -M_D\nabla\left(\frac{T_0}{T}\mu - \varepsilon^2\nabla^2 x\right). \tag{12}$$

The coefficients $M_T > 0$ and $M_D > 0$ are positive flux mobilities.

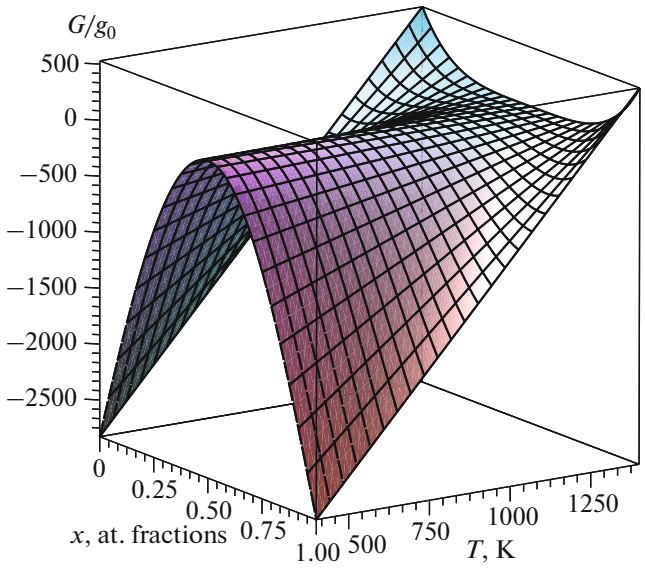

Fig. 1. (Color online) The Ginzburg–Landau energy (15) as a function of temperature T and the impurity concentration x.

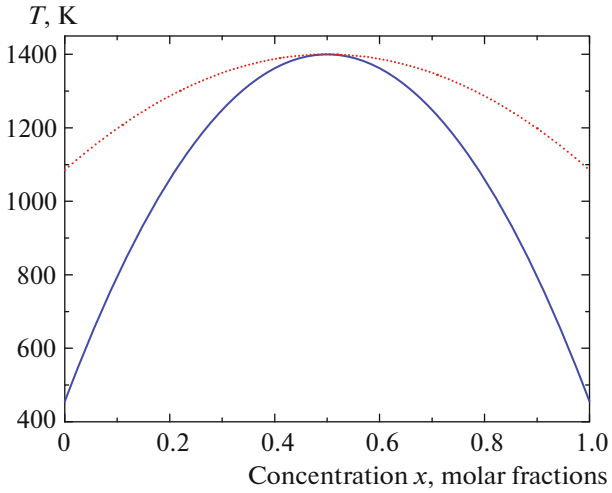

Fig. 2. (Color online) (dashed curve) Binodal and (solid curve) spinodal of the Ginzburg–Landau potential (15).

As a result, we find that the dynamics of spinodal decomposition taking into account the continuous variation of temperature is governed by a coupled system of equations including the Cahn–Hilliard equation modified by the effective chemical potential

$$\mu_{\text{eff}}(T,x) = \mu\frac{T_0}{T}, \tag{13}$$

$$\frac{\partial x}{\partial t} = \nabla\cdot[M_D\nabla(\mu_{\text{eff}}(T,x) - \varepsilon^2\nabla^2 x)] \tag{14}$$

and the heat equation (7) with flux (11).

5. THERMODYNAMIC POTENTIAL

To qualitatively study the effect of nonisothermality on spinodal decompositrion, we take the volume density of the Gibbs energy as the Ginzburg–Landau model potential [43]

$$\frac{G(T,x)}{g_0} = \left(\frac{T}{T_c} - 1\right)(x - x_c)^2 + B_0(x - x_c)^4. \tag{15}$$

As the parameters of the Gibbs potential, we use $g_0 = 1.88\times 10^4$ J/cm^3, $B_0 = 0.45$, $x_c = 0.5$, and $T_c = 1400$ K, which are chosen for illustrative purposes. The corresponding surface of the Gibbs energy is demonstrated in Fig. 1. In view of the symmetry of the potential with respect to concentration, the binodal and spinodal of the model system are defined by the conditions $(\partial G/\partial x)_T = 0$ and $(\partial^2 G/\partial x^2)_T = (\partial\mu/\partial x)_T = 0$. The graphs of the binodal and spinodal are demonstrated in Fig. 2.

6. INITIAL STAGES OF NONISOTHERMAL SPINODAL DECOMPOSITION

Consider an idealized situation when a solution with average concentration $\bar{x}$ and temperature T_0 is very rapidly (instantaneously) cooled to temperature $\bar{T}$, which is then maintained constant at the boundaries of the sample. We will assume that, at the initial instant of time, the fluctuations of the initial composition and the initial temperature distribution are so small that one can neglect the spatial derivatives of the specific heat C_p, heat conductivity λ, the diffusion coefficient D_0, as well as the derivatives of the chemical potential $\partial\mu/\partial x$ and $\partial(\mu T)/\partial T$.

Introducing the thermal diffusivity a, $a = \kappa/C_p$, and the diffusion coefficient D_0,

$$D_0 = M_D\mu_x, \quad \text{where} \quad \mu_x \equiv \frac{\partial\mu}{\partial x}, \tag{16}$$

we rewrite Eqs. (7) and (14) as

$$\begin{gathered}\frac{\partial x}{\partial t} = -|D_0|\frac{T_0}{T}\nabla^2 x + \left|\frac{D_0}{\mu_x}\right|\left(T_0\frac{\partial}{\partial T}\left(\frac{\mu}{T}\right)\nabla^2 T - \varepsilon^2\nabla^4 x\right),\\ \frac{\partial T}{\partial t} = a\nabla^2 T + \frac{T^2}{C_p}\frac{\partial x}{\partial t}\frac{\partial}{\partial T}\left(\frac{\mu}{T}\right).\end{gathered} \tag{17}$$

Here it is assumed that the initial concentration $\bar{x}$ and the (instantaneous) temperature $T(\mathbf{r}, t)$ correspond to the spinodal domain for the Gibbs potential $G(T, x)$; i.e., for a given $\bar{x}$, the temperature T is below the critical value:

$$T < T_c[1 - 6B_0(\bar{x} - x_c)^2].$$

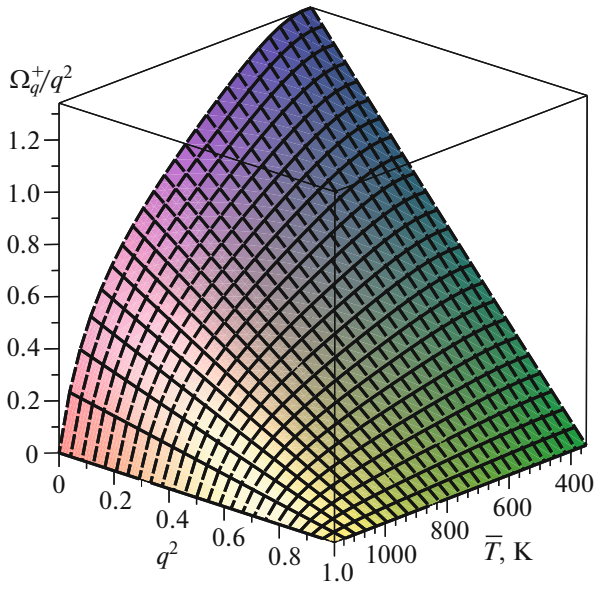

Fig. 3. (Color online) Q_q^+/q^2 as a function of the squared wave number q^2 and temperature $\overline{T}$.

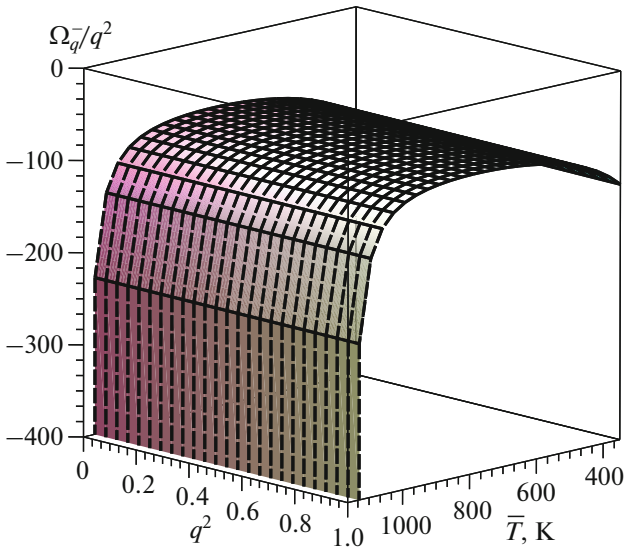

Fig. 4. (Color online) Q_q^-/q^2 as a function of the squared wave number q^2 and temperature.

7. FOURIER ANALYSIS

Consider a one-dimensional problem of evolution of initial stages of spinodal decomposition in an unbounded domain with space coordinate z. The deviations of concentration and temperature from their average values at any instant of time can be expressed in terms of the Fourier components (x_k, T_k) as

$$\begin{pmatrix} x-\overline{x} \\ T-\overline{T} \end{pmatrix} = \sum_k \begin{pmatrix} x_k \\ T_k \end{pmatrix} e^{\omega t+ikz}, \tag{18}$$

where ω is the frequency of the Fourier harmonic with wave number k.

The substitution of the Fourier expansion (18) into Eq. (17) leads to the following dispersion relation:

$$\begin{aligned}(\omega + ak^2)\left[\omega - \frac{T_0}{\overline{T}}|D_0|k^2\left(1-\frac{\overline{T}}{T_0}\frac{\varepsilon^2}{|\mu_x|}k^2\right)\right] \\ + \tilde{\mu}^2\frac{|D_0|}{|\mu_x|}\frac{\overline{T}^2T_0}{C_p}\omega k^2 = 0,\end{aligned} \tag{19}$$

where

$$\tilde{\mu} = \frac{\partial}{\partial T}\left(\frac{\mu}{T}\right)\Bigg|_{T=\overline{T}}.$$

After the change

$$\begin{aligned}k^2 &= q^2\frac{|\mu_x|}{\varepsilon^2}\frac{T_0}{\overline{T}}, \\ \omega &= \Omega|D_0|\frac{|\mu_x|}{\varepsilon^2}\frac{T_0}{\overline{T}},\end{aligned} \tag{20}$$

where $\sqrt{|\mu_x|T_0/\varepsilon^2T}$ and $|D_0\mu_x|T_0/\varepsilon^2\overline{T}$ are the characteristic scales of the wave number and frequency, as well as using the notation $\tau = |D_0|/a$, we can easily reduce the dispersion relation (19) to the quadratic equation

$$\begin{aligned}\tau\Omega^2 + \Omega q^2\left(1-\tau\frac{T_0}{\overline{T}}(1-q^2)+\tau\tilde{\mu}^2\frac{\overline{T}^2T_0}{C_p|\mu_x|}\right) \\ -\frac{T_0}{\overline{T}}(1-q^2)q^4 = 0.\end{aligned} \tag{21}$$

Now, calculating the discriminant of Eq. (21),

$$D = \left[1-\tau\frac{T_0}{\overline{T}}(1-q^2)+\tau\tilde{\mu}^2\frac{\overline{T}^2T_0}{C_p|\mu_x|}\right]^2 + 4\tau\frac{T_0}{\overline{T}}(1-q^2),$$

we find the roots of the quadratic equation:

$$\Omega_q^{\pm} = -\frac{q^2}{2\tau}\left[1-\tau\frac{T_0}{\overline{T}}(1-q^2)+\tau\tilde{\mu}^2\frac{\overline{T}^2T_0}{C_p|\mu_x|}\pm\sqrt{D}\right]. \tag{22}$$

The dependence of $\Omega_q^{\pm}/q^2$ on temperature and wave number is demonstrated in Figs. 3 and 4 for the following values of the parameters: the initial concentration of the solution $\overline{x} = 0.25$, the initial temperature of the solution $T_0 = 1410$ K, the parameter $\varepsilon = 6.2 \times 10^{-8}$ (J/cm)$^{1/2}$, the diffusion coefficient $|D_0| = 5.5 \times 10^{-5}$ cm^2/s, the thermal diffusivity $a = 2.2 \times 10^{-3}$ cm^2/s, and the specific heat $C_p = 0.5$ J/(cm^3 K). Figures 3 and 4 show that the increasing solutions correspond only to Ω_q^+, whereas Ω_q^- is always negative and defines decaying harmonics.

Figure 3 also shows that Ω_q^+/q^2 is a linear function of q^2 for any fixed temperature and reproduces the function $\Omega(q)/q^2$ for the Cahn–Hilliard model in the

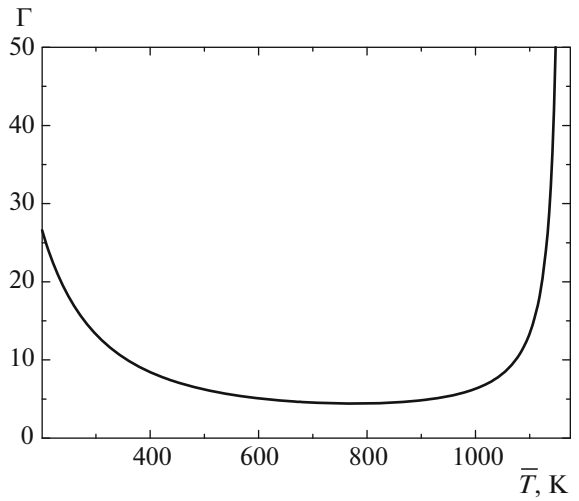

Fig. 5. The dimensionless parameter Γ as a function of the average temperature $\bar{T}$ for the Ginzburg–Landau potential for $\bar{x} = 0.25$.

isothermal situation. Therefore, one would think that such a situation also should contradict the experimental data [10]. However, the similarity between these two functions should not be misleading. The full solution of the nonisothermal model, in contrast to the Cahn–Hilliard model, is determined by the superposition of two independent solutions corresponding to both Ω_q^+ and Ω_q^- (see Fig. 4). Therefore, the growth dynamics of initial perturbations in the nonisothermal model may essentially differ from that in the Cahn–Hilliard model.

It is easily seen that the Cahn–Hilliard model arises for dispersion (22) only in two limit situations. Indeed, for finite values of thermal diffusivity, the parameter τ is a small but finite quantity. In the case of very high thermal diffusivity ($a \to \infty$), after the division of Eq. (17) by the coefficient a, there remains a single physically reasonable solution in the form $\bar{T} = \text{const}$ on the infinite interval. In the limit of $\tau \to 0$, the dispersion equation (21) reduces, up to a temperature factor, to a linear (in q^2) Cahn–Hilliard dispersion law:

$$\frac{\Omega_q}{q^2} = \frac{T_0}{\bar{T}}(1 - q^2). \tag{23}$$

A more interesting situation is related to the fact that the Cahn–Hilliard dispersion can be obtained by examining the contribution of the term proportional to $\bar{T}^2/C_p$ to the dispersion equation (22). The emergence of such a dimensionless factor is by no means accidental because, following [44], one can easily show that, in the isobaric case, $\bar{T}^2/C_p$ is the variance of temperature fluctuations in a canonical ensemble (see the Appendix), whence

$$\Gamma \equiv \frac{\bar{T}^2}{C_p}\frac{\tau T_0}{|\mu_x|}\tilde{\mu}^2 \propto \langle(\Delta T)^2\rangle.$$

The limit $\Gamma \to 0$ corresponds to the limit of small temperature fluctuations, because, as a result, the initial dispersion relation (19) reduces to the product of factors

$$(\omega + ak^2)\left[\omega - \frac{T_0}{\bar{T}}|D_0|k^2\left(1 - \frac{\bar{T}}{T_0}\frac{\varepsilon^2}{|\mu_x|}k^2\right)\right] = 0,$$

which determine the dispersion of two independent equations (the heat equation and the Cahn–Hilliard equation). The Cahn–Hilliard equation, which arises in the limit of $\Gamma \to 0$, contains only the average temperature, which redefines the diffusion coefficient, whereas temperature fluctuations have no effect on spinodal decomposition.

Conversely, under the condition $\Gamma \gg 1$, one cannot neglect the contribution of thermal fluctuations, because we have a strongly coupled system of equations in which thermal noise should play an important role. The emergence of thermal fluctuations $\langle\Delta T^2\rangle$ in the dispersion relation (22) can be interpreted as a result of averaging the dynamics of spinodal decomposition with respect to random external forces. Physically, the emergence of random forces occurs due to the local variation of the impurity concentration, which is responsible for the fluctuating source in the heat equation (17) normalized by the variance of temperature fluctuations. Usually, $\tau \ll 1$; therefore, heat propagation processes occur much faster than diffusion processes and give rise to rapidly varying heat fluxes that play, according to Cook's idea [7], the role of random forces in the equation for concentration.

Thus, taking into account random fluctuations, as is done in the LBM model [8] to match to experimental data, arises naturally within the nonisothermal model of spinodal decomposition. Moreover, the Fourier analysis shows that the values of the dimensionless parameter Γ can serve a certain criterion for the necessity to take into account temperature fluctuations in the system. In particular, for binary systems, the Γ criterion can be calculated on the basis of open thermodynamic database NIMS [45]. For the Ginzburg–Landau potential considered in the present study, the dependence of Γ on the average temperature $\bar{T}$ for a given concentration $\bar{x} = 0.25$ is shown in Fig. 5. At temperatures close to the spinodal boundary, $\Gamma \to \infty$ because the boundary is defined as

$$\frac{\partial^2 G}{\partial x^2} \equiv \frac{\partial \mu}{\partial x} \equiv \mu_x = 0 \Rightarrow \Gamma = \frac{\bar{T}^2}{C_p}\frac{\tau T_0}{|\mu_x|}\tilde{\mu}^2 \to \infty.$$

As temperature $\bar{T}$ decreases, the parameter Γ again starts to monotonically increase after some plateau. From Fig. 5 we can conclude that temperature fluctuations should especially strongly manifest themselves at the intersection of spinodal boundaries and (much

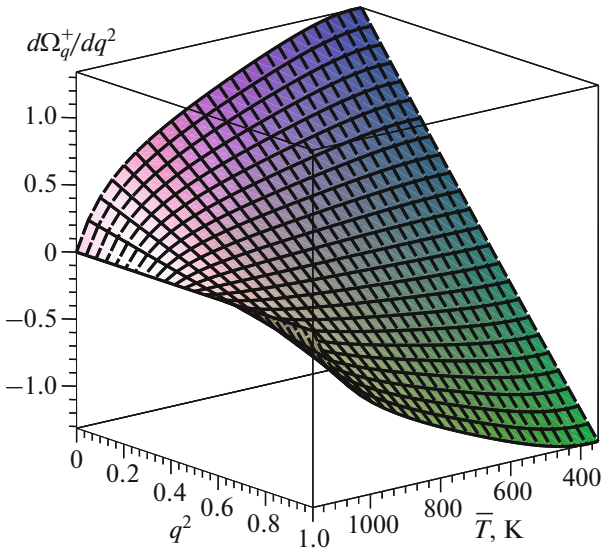

Fig. 6. (Color online) The derivative $d\Omega_q^+/dq^2$ as a function of the average temperature $\overline{T}$ and the squared wave number q^2.

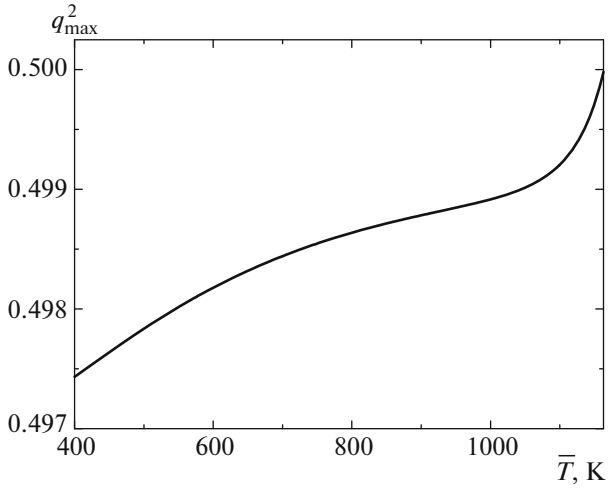

Fig. 7. The squared wave number $q^2_{\max}$ as a function of the average temperature $\overline{T}$.

weaker) at sufficiently low temperatures. Since the cooling process is not instantaneous in practice, temperature fluctuations should manifest themselves precisely at early stages of spinodal decomposition and remain insignificant at large times.

The difference in the behavior of isothermal and nonisothermal Cahn–Hilliard models is already seen from the analysis of the maximally unstable Fourier mode. The surface of the derivative $d\Omega_q^+/dq^2$ from the solution of (22) is demonstrated in Fig. 6. Solving the equation $d\Omega_q^+/dq^2 = 0$, we find that the wave number corresponding to the maximum instability varies (although rather slowly for chosen parameters of the model) under the variation of the average temperature, in contrast to the constant maximum in the isothermal Cahn–Hilliard model. The corresponding dependence is demonstrated in Fig. 7.

8. STRUCTURE FACTOR OF THE NONISOTHERMAL MODEL

For simplicity, we will assume that there are no temperature fluctuations at the initial moment, $T_q^{(0)} = 0$, and the composition fluctuations have the same magnitude for all Fourier components: $x_q^{(0)} = \text{const}$. We take unnormalized eigenvectors corresponding to $\Omega_\pm$ in the form

$$\mathbf{v}_q^\pm = \begin{pmatrix} 1 \\ \dfrac{\tilde{\mu}\overline{T}^2}{\left(1+\dfrac{q^2}{\tau\Omega_q^\pm}\right)C_p} \end{pmatrix}, \qquad (24)$$

and the general solution for a Fourier harmonic q has the form

$$\begin{pmatrix} x_q \\ T_q \end{pmatrix} = A_q\mathbf{v}_q^+ e^{\omega_q^+ t' + iqz'} + B_q\mathbf{v}_q^- e^{\omega_q^- t' + iqz'}, \qquad (25)$$

where t' and z' are dimensionless time and coordinate related to t and z by the scale change (20). Since $\exp(\omega^+ t)$ appears in both variables (T, x), the instability determining the spinodal decomposition manifests itself in a local increase in the temperature field due to the source ($\propto \partial x/\partial t$) in the heat equation (17). Using the initial conditions, we obtain the following system of equations for the coefficients A_q and B_q:

$$\begin{gathered} A_q + B_q = x_q^{(0)}, \\ \frac{A_q}{1+q^2/\tau\Omega_q^+} + \frac{B_q}{1+q^2/\tau\Omega_q^-} = 0. \end{gathered} \qquad (26)$$

Calculating the Fourier amplitudes from system (26) and defining the structure factor as $S_q(t) = N_q^{-1}|x_q(t)|^2$, we can easily calculate the time evolution of the structure factor. The normalization coefficient is taken equal to $N_q = |x_q(0)|^2$. The corresponding graphs for different temperatures are presented in Figs. 8–10. These graphs show that the formation rate of a periodic spinodal structure significantly increases as temperature decreases.

Note that the structure factor in Figs. 8–10 is presented for sufficiently large dimensionless times, which actually correspond to the late stages of spinodal decomposition. Although the average temperature is almost constant at such times in view of the chosen boundary conditions, the impurity distribution becomes highly inhomogeneous, which is indicated by the structure factor itself. In view of the lin-

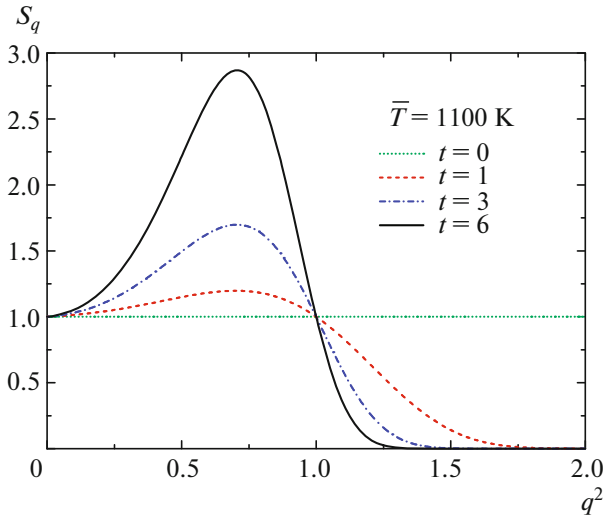

Fig. 8. (Color online) Structure factor S_q as a function of the squared wave number q^2 at different instants of time t at temperature $\overline{T} = 1100$ K.

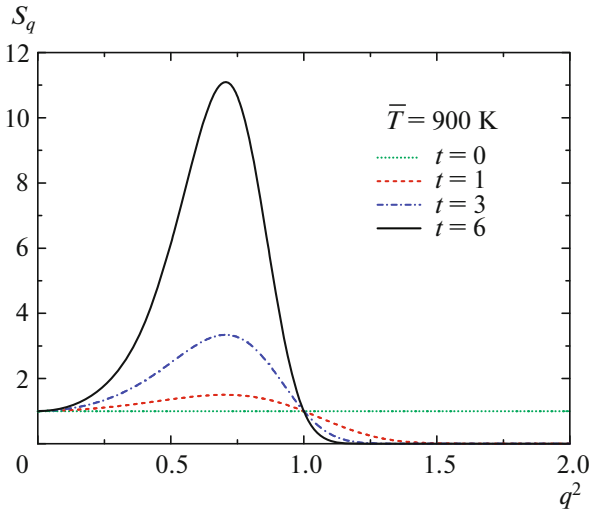

Fig. 9. (Color online) Structure factor S_q as a function of the squared wave number q^2 at different instants of time t at temperature $\overline{T} = 900$ K.

earization of the problem for the Fourier analysis, its solutions can be assumed valid up to times of $t_0 \approx 1/\Omega_q^+$; at large times $t > t_0$, we need a numerical analysis of the whole nonlinear problem (17). Therefore, here the graphs (Figs. 8–10) are presented for illustrative purposes, to show the dependence of the spinodal decomposition process on the average temperature $\overline{T}$. One can expect that the nonlinearity of the problem introduces some changes in the form of the structure factor at late stages; however, the qualitative dependence of the structure factor on q^2 changes rather weakly, because the wormlike structure of impurity distribution by the time t_0 will be close to the stationary state.

9. GROWTH RATE

The growth rate $R(q^2, t)$, more precisely, $R(q^2, t)/q^2$, defined as

$$R(q^2,t) = \frac{1}{S_q}\frac{dS_q}{dt}, \qquad (27)$$

and measured in experiments, is an important characteristic of spinodal decomposition. The growth rate for the Cahn–Hilliard equation is easily determined from the dispersion equation

$$R(q^2,t)q^{-2} = 2(1-q^2). \qquad (28)$$

This equation is linear in q^2 and is independent of time. The real graph of $R(q^2, t)/q^2$ is demonstrated in Fig. 11. The dependence of $R(q)q^{-2}$ on q^2 for a solid solution of Al–12.1 at % Zn at temperature of $\overline{T} = 293$ K [46, 47] exhibits strong nonlinearity and dependence on time. Since the difference between (28) and the functions in Fig. 11 is what makes the main difference between theory and experiment, we consider the growth rate within the nonisothermal model. For comparison, we produce the graphs of the growth rate in Figs. 12 and 13. Both figures correspond to the same parameters of the model, except for the parameter Γ, which takes a value of $\Gamma_1 = 66.44 \times 10^2$ in Fig. 12 and a value of $\Gamma_2 = 66.44$ in Fig. 13. The parameter Γ_1 is chosen from considerations of similarity with Fig. 11, while the parameter $\Gamma_2 = 0.01\Gamma_1$ in Fig. 13 is chosen to demonstrate the effect of Γ on the growth rate. In par-

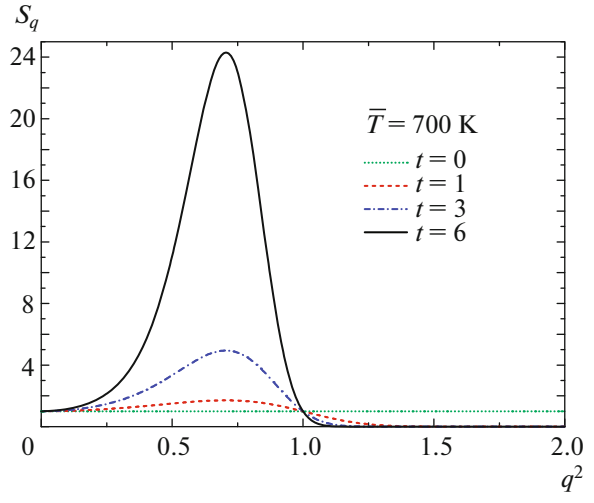

Fig. 10. (Color online) Structure factor S_q as a function of the squared wave number q^2 at different instants of time t at temperature $\overline{T} = 700$ K.

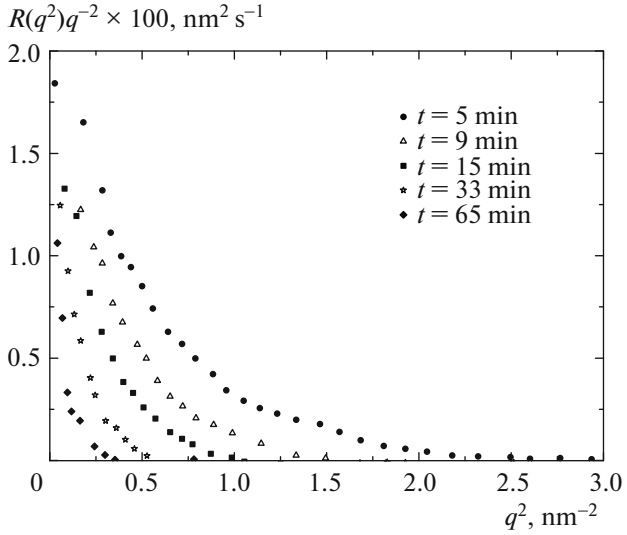

Fig. 11. Typical experimental values of the growth rate $R(q)q^{-2}$ as a function of q^2 for Al–12.1 at % Zn at different instants of time t at an average temperature of $\overline{T} = 293$ K [46, 47].

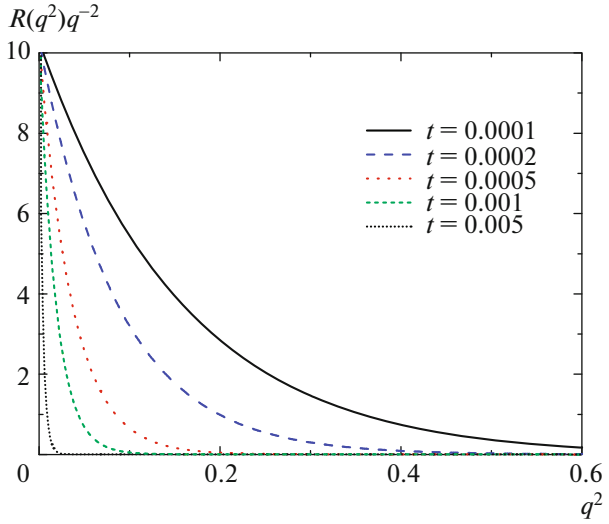

Fig. 12. (Color online) Theoretical values of the growth rate $R(q)q^{-2}$ as a function of q^2 at different instants of time t at an average temperature of $\overline{T} = 300$ K and $\Gamma = 66.44 \times 10^2$.

ticular, Fig. 12 shows that the model of nonisothermal spinodal decomposition can qualitatively describe experimental data for real systems. We did not carry out a quantitative comparison of the nonisothermal model with the results of [46, 47] due to the lack of detailed information on the experiment and on the thermophysical data of materials in the open literature. Note also that the graphs in Fig. 12 correspond to small dimensionless times, when the linear approximation (and the corresponding Fourier series expansion) in the nonisothermal model is quite valid.

10. CONCLUSIONS

In this work, based on the principle of increasing entropy, we have obtained a nonisothermal generalization of the Cahn–Hilliard model of spinodal decomposition, which is based on the joint dynamics of the concentration field $x(\mathbf{r}, t)$ and the temperature field $T(\mathbf{r}, t)$.

The analysis of the early stages of spinodal decomposition has shown that the effect of nonisothermality on the impurity dynamics is not reduced only to taking into account random forces, as considered in the earlier works [7, 8]. The nature of the interaction between temperature variations and spinodal decomposition turns out to be much more complicated than it was assumed in these works and manifests itself in a nonlinear change in the dispersion relation, determined by the parameter $\tau = |D_0|/a$ and the dimensionless quantity related to temperature fluctuations $\Gamma \propto \langle \Delta T^2 \rangle$. Only in the case of sufficiently large thermal diffusivity (with respect to the diffusion coefficient) or a small parameter Γ, as can be seen from the comparison of Figs. 12 and 13, the dependence $R(q^2)q^{-2}$ becomes close to linear. Moreover, the parameter Γ can be considered as a certain criterion indicating the need to take into account nonisothermality. Since any system in a real process passes through lability bounds during supercooling, Γ always takes large values at such times; therefore, the classical Cahn–Hilliard equation can be used to describe and simulate spinodal decomposition

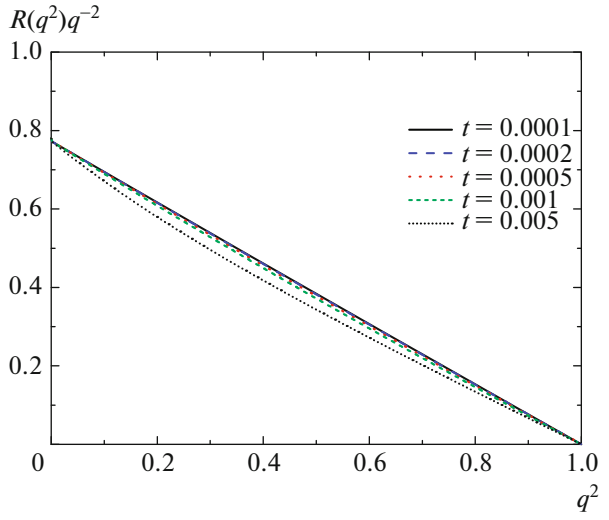

Fig. 13. (Color online) Theoretical values of the growth rate $R(q)q^{-2}$ as a function of q^2 at different instants of time t at an average temperature of $\overline{T} = 300$ K and $\Gamma = 66.44$.

without taking temperature fluctuations into account only in some ideal situations.

Even without taking into account the differences in the dispersion behavior of the proposed nonisothermal model compared to the LBM or CHC approaches, from a purely computational point of view, this nonisothermal model has a significant advantage in the computer simulation of spinodal decomposition. This is determined by the fact that the process of simultaneous solution of the spinodal decomposition equations (14) with the heat equation (7) and (11) allows one to solve the simulation problem as a fully deterministic problem, without requiring the averaging of results over a random source, which is necessary in the LBM or CHC models.

In this work, we have investigated only the effect of nonisothermicity on temperature variations in a solution on the dynamics of spinodal decomposition. However, there are other factors that influence spinodal decomposition: the Brownian motion of droplets with different concentrations [22] followed by their agglomeration, the emergence of metastable nuclei of a new phase when supercooling the solution that compete with the process of spinodal decomposition, the appearance of internal stresses (in solid solutions), and other concomitant phenomena. Since the effect of such factors has been studied rather poorly, both the development of experimental methods for studying spinodal decomposition and the extension of theoretical models by the inclusion of new phenomena remain topical.

Since the nonisothermal model of spinodal decomposition is more general compared with the classical Cahn–Hilliard model and includes the latter as a special case, it should be applicable to the late stages of spinodal decomposition. However, the question of to what effects can nonisothermality lead in the description of the spinodal decomposition problem at its late stages should be solved in a separate study based on numerical simulation. Such a numerical study and the subsequent comparison with experiment are also relevant for the early stages of spinodal decomposition.

APPENDIX

PROBABILITY OF FLUCTUATIONS IN A CANONICAL ENSEMBLE

Probability of fluctuation in a canonical ensemble is defined by relation (112.3) from [44]:

$$\omega \propto \exp\left(\frac{\Delta P\Delta V - \Delta T\Delta S}{2T}\right).$$

From this general formula, we can find the fluctuations of various thermodynamic quantities. In the textbook [44], the authors took V and T as variables, because they are independent random variables. We take P and T as the variables. Then

$$\Delta S = \left(\frac{\partial S}{\partial T}\right)_P \Delta T + \left(\frac{\partial S}{\partial P}\right)_T \Delta P = \frac{C_p}{T}\Delta T - \left(\frac{\partial V}{\partial T}\right)_P \Delta P,$$

$$\Delta V = \left(\frac{\partial V}{\partial T}\right)_P \Delta T + \left(\frac{\partial V}{\partial P}\right)_T \Delta P.$$

The fluctuation probability is determined by the expression

$$\Delta P\Delta V - \Delta T\Delta S = \left[\left(\frac{\partial V}{\partial T}\right)_P \Delta T + \left(\frac{\partial V}{\partial P}\right)_T \Delta P\right]\Delta P - \left[\frac{C_p}{T}\Delta T - \left(\frac{\partial V}{\partial T}\right)_P \Delta P\right]\Delta T$$

$$= -\frac{C_p}{T}\Delta T^2 + \left(\frac{\partial V}{\partial P}\right)_T \Delta P^2 + 2\left(\frac{\partial V}{\partial T}\right)_P \Delta T\Delta P.$$

Thus, the fluctuations ΔT and ΔP are correlated; however, for the isobaric system considered in this paper, the fluctuations of pressure are missing in principle, $\Delta P \equiv 0$; therefore, the probability of temperature fluctuations is

$$\omega \propto \exp\left(-\frac{C_p}{T^2}\Delta T^2\right).$$

This implies that the variance of temperature fluctuations for a canonical ensemble in the variables P and T is given by

$$\langle(\Delta T)^2\rangle = \frac{T^2}{C_p}.$$

Note also the fact that the present study is "invariant" with respect to a change of isochoricity to isobaricity, because these characteristics are nowhere used. Therefore, announcing the free energy as a control potential, we could obtain formula (112.6) from [44], which differs by the change $C_p \to C_V$ in the expression for the variance of temperature fluctuations. The Ginzburg–Landau potential can be assumed to be both the free energy and the Gibbs potential because it is independent of volume and pressure. In the present study, the choice of the term "Gibbs potential" for the Ginzburg–Landau potential and, hence, the isobaricity of the system are related solely to the fact that the description of the thermodynamics of real materials [32, 45] is based on the Gibbs potentials.

FUNDING

This work was supported by the Russian Foundation for Basic Research and the Government of the Udmurt Republic (project no. 18-42-180002), as well as in part by the Russian Foundation for Basic Research (project no. 18-02-00643) and the German Space Center Space Management (contract no. 50WM1541).

REFERENCES

1. N. Jinnai, T. Hashimoto, D. Lee, et al., Macromolecules **30**, 130 (1997).
2. F. Mallamace, N. Micali, and S. Trusso, J. Phys.: Condens. Matter **8**, A81 (1996).
3. N. F. Bunkin, A. V. Lobeev, and G. A. Lyakhov, Phys. Usp. **40**, 1019 (1997).
4. J. Mainville, Y. S. Yang, K. R. Elder, et al., Phys. Rev. Lett. **78**, 258 (1997).
5. J. W. Cahn and J. E. Hilliard, J. Chem. Phys. **28**, 258 (1958).
6. J. W. Cahn, Acta Metall. **9**, 795 (1961).
7. N. E. Cook, Acta Metall. **18**, 297 (1970).
8. J. S. Langer, M. Baron, V. P. Skripov, A. V. Skripov, and H. D. Miller, Phys. Rev. A **11**, 1417 (1975).
9. V. P. Skripov and A. V. Skripov, Sov. Phys. Usp. **22**, 389 (1979).
10. K. Binder and P. Fratzl, in *Phase Transformations in Materials*, Ed. by G. Kostorz (Wiley-VCH, Weinheim, 2001), p. 409.
11. N. S. Andreev, G. G. Boiko, and N. A. Bokov, J. Non-Cryst. Solids **5**, 41 (1970).
12. N. S. Andreev and E. A. Porai-Koshits, Discuss. Faraday Soc. **50**, 135 (1970).
13. K. Binder, Phys. Rev. A **29**, 341 (1984).
14. M. Laradji, M. Grant, M. J. Zuckennann, et al., Phys. Rev. B **41**, 4646 (1990).
15. E. D. Siggia, Phys. Rev. A **20**, 595 (1979).
16. P. Galenko, Phys. Lett. A **287**, 190 (2001).
17. P. Galenko and D. Jou, Phys. Rev. E **71**, 046125 (2005).
18. P. Galenko and D. Jou, Phys. A (Amsterdam, Neth.) 388, 3113 (2009).
19. P. Galenko and V. Lebedev, Philos. Mag. Lett. **87**, 821 (2007).
20. P. K. Galenko and V. G. Lebedev, JETP Lett. **86**, 458 (2007).
21. N. Lecoq, H. Zapolsky, and P. Galenko, Eur. Phys. J. Spec. Top. **177**, 165 (2009).
22. A. Oprisan, S. A. Oprisan, J. J. Hegseth, et al., Phys. Rev. E **77**, 051118 (2008).
23. E. L. Huston, J. W. Cahn, and J. E. Hilliard, Acta Metall. **14**, 1053 (1966).
24. H. W. Alt and I. Pawlow, Phys. D (Amsterdam, Neth.) 59, 389 (1992).
25. A. Miranville and G. Schimperna, Discr. Cont. Dyn. Syst. B **5**, 753 (2005).
26. M. Krivilyov, D. Aflyatunova, V. G. Lebedev, and P. K. Galenko, Comput. Mater. Sci. **158**, 289 (2019).
27. D. A. Danilov, V. G. Lebedev, and P. K. Galenko, J. Non-Eq. Therm. **39**, 93 (2014).
28. H. Risken, in *The Fokker–Planck Equation: Methods of Solutions and Applications* (Springer, Berlin, 1984), p. 452.
29. A. E. Bailey and D. S. Canell, Phys. Rev. Lett. **70**, 2110 (1993).
30. J. P. Donley and S. Langer, Phys. Rev. Lett. **71**, 1573 (1993).
31. J. Mainville, Y. S. Yang, K. R. Elder, et al., Phys. Rev. Lett. **78**, 2787 (1997).
32. M. Hillert, *Phase Equilibria, Phase Diagrams and Phase Transformations: Their Thermodynamic Basis* (Cambridge Univ. Press, New York, 2008), p. 510.
33. H. Zapolsky, C. Pareige, L. Marteau, D. Blavette, and L. Q. Chen, CALPHAD **25**, 125 (2001).
34. D. J. Seol, S. Y. Hu, Y. L. Li, J. Shen, K. H. Oh, and L. Q. Chen, Met. Mater. Int. **9**, 61 (2003).
35. S. Lezama-Alvareza, E. O. Avila-Davilab, V. M. Lopez-Hirataa, et al., Mater. Res. **16**, 975 (2013).
36. S. Dai and Q. Du, J. Comp. Phys. **310**, 85 (2016).
37. J. Kim, S. Lee, Y. Choi, et al., Math. Probl. Eng. 2016, 9532608 (2016). https://doi.org/10.1155/2016/9532608
38. A. R. Balakrishna and W. C. Carter, Phys. Rev. E **97**, 043304 (2018).
39. J. D. Gunton, R. Toral, and A. Chakrabarti, Europhys. Lett. T **33**, 12 (1990).
40. J. García-Ojalvo, A. M. Lacasta, J. M. Sancho, et al., Europhys. Lett. **42**, 125 (1998).
41. P. Gera and D. Salac, R. Soc. Open Sci. **4**, 170472 (2017). https://doi.org/10.1098/rsos.170472
42. S. R. de Groot and P. Mazur, *Non-Equilibrium Thermodynamics* (North-Holland, Amsterdam, 1962).
43. E. P. Feldman and L. I. Stefanovich, Sov. Phys. JETP **71**, 951 (1990).
44. L. D. Landau and E. M. Lifshitz, *Course of Theoretical Physics*, Vol. 5: *Statistical Physics* (Fizmatlit, Moscow, 2005; Pergamon, Oxford, 1980).
45. http://cpddb.nims.go.jp/cpddb/periodic.htm. Accessed August 25, 2018.
46. P. Guyot and J. P. Simon, in *Proceedings of the International Conference on Solid–Solid Phase Transformations*, Ed. by H. I. Aaronson (Met. Soc. of AIME, 1983), p. 325.
47. K. Hono and K.-I. Hirano, Phase Trans. **10**, 223 (1987).

Translated by I. Nikitin